THE ASTROPHYSICAL JOURNAL, 495:786–795, 1998 March 10
© 1998. The American Astronomical Society. All rights reserved. Printed in U.S.A.

TWO-COMPONENT FOKKER-PLANCK MODELS FOR THE EVOLUTION OF ISOLATED GLOBULAR CLUSTERS

SUNGSOO S. KIM[1]
Institute for Basic Sciences, Pusan National University, Pusan 609-735, Korea; sskim@uju.es.pusan.ac.kr
HYUNG MOK LEE
Department of Earth Sciences, Pusan National University, Pusan 609-735, Korea; hmlee@uju.es.pusan.ac.kr
AND
JEREMY GOODMAN
Princeton University Observatory, Peyton Hall, Princeton, NJ 08544; jeremy@astro.princeton.edu
Received 1997 June 30; accepted 1997 October 16

ABSTRACT

Two-component (normal and degenerate stars) models are the simplest realization of clusters with a mass spectrum because high-mass stars evolve quickly into degenerates, while low-mass stars remain on the main sequence for the age of the universe. Here we examine the evolution of isolated globular clusters by using two-component Fokker-Planck (FP) models that include heating by binaries formed in tidal capture and in three-body encounters. Three-body binary heating dominates, and the postcollapse expansion is self-similar, at least in models with total mass $M \leq 3 \times 10^5\ M_\odot$, initial half-mass radius $r_{h,i} \geq 5$ pc, component mass ratio $m_2/m_1 \geq 2$, and number ratio $N_1/N_2 \leq 300$, when $m_2 = 1.4\ M_\odot$. We derive scaling laws for ρ_c, v_i, r_c, and r_h as functions of m_1/m_2, N, M, and time t from simple energy-balance arguments; these agree well with the FP simulations. We have studied the conditions under which gravothermal oscillations (GTOs) occur. If $E_{\rm tot}$ and E_c are the energies of the cluster and of the core, respectively, and $t_{\rm rh}$ and t_c are their relaxation times, then $\epsilon \equiv (E_{\rm tot}/t_{\rm rh})/(E_c/t_{\rm rc})$ is a good predictor of GTOs: all models with $\epsilon > 0.01$ are stable, and all but one with $\epsilon < 0.01$ oscillate. We derive a scaling law for ϵ against N and m_1/m_2 and compare them with our numerical results. Clusters with larger m_2/m_1 or smaller N are stabler.

Subject headings: celestial mechanics, stellar dynamics — globular clusters: general

1. INTRODUCTION

The dynamical evolution of pre- and postcollapse globular clusters is influenced by many factors: the initial mass function, the nature and efficiency of energy generation mechanisms, galactic tides, anisotropy of the velocities, the initial population of binaries, and stellar evolution (see, e.g., Spitzer 1987). If the goal is to model globular clusters realistically, then all of these effects should be included. On the other hand, if the goal is a deeper theoretical understanding of individual dynamical processes, then simpler models can be more instructive.

A distribution of stellar masses affects the postcollapse evolution of globular clusters in ways that have not been fully explored. The simplest nontrivial multimass models are those with just two components. This simplification is drastic but not entirely unrealistic. Since the stellar main-sequence lifetime is a very steep function of stellar mass, a cluster can be assumed to start its dynamical evolution with a turnoff-point mass very similar to that currently observed. Stars with higher mass have already evolved into degenerate remnants (such as black holes, neutron stars, or white dwarfs). Because of mass segregation (also called "mass stratification"; cf. Spitzer 1987), the inner parts of a dynamically relaxed cluster should consist primarily of the turnoff stars and the heaviest remnants. The black holes are probably much more massive than present-day main-sequence stars, but their number is expected to be too small to play any important dynamical role (Kulkarni, Hut, & McMillan 1993). Most of the white dwarfs in a cluster are expected to have masses less than the present turnoff point mass. The dynamical effects of such white dwarf stars are expected to be unimportant. Kim & Lee (1997) compared the numerical results of two- and 11-component models, which have three components for the white dwarfs heavier than the turnoff-point mass, and they were able to find two-component cluster parameters that well match the 11-component clusters. This implies that the presence of the white dwarfs heavier than the turnoff-point mass does not harm the two-component approximation.

Neutron stars, however, can be an important component in dynamical evolution of globular clusters. Neutron stars are about twice as massive as turnoff stars. The fraction of the cluster mass in the form of neutron stars is expected to be very small, but mass segregation may make neutron stars a major component in the central parts. (For observational evidence supporting the dominance of heavy degenerates, see Gebhardt & Fischer 1995 and Phinney 1993). As a first approximation, the globular clusters can be represented by two components: neutron stars and main-sequence stars.

Two-component clusters have several interesting features that are not present in single-component clusters. Mass segregation significantly accelerates the early phases of core collapse (e.g., Yoshizawa et al. 1978; Inagaki & Wiyanto 1984; Spitzer 1987). The central parts quickly become dominated by a heavy component, even though the bulk of the mass of the cluster is in the light component. Tidal captures between a neutron star and a main-sequence star are frequent, and binaries composed of neutron stars can also be formed by three-body processes. These binaries will eventually drive the postcollapse evolution.

[1] Present address: Department of Physics, Space Science Laboratory, Korea Advanced Institute of Science & Technology, Daejon 305-701, Korea.

The purpose of this paper is to obtain a series of solutions for the dynamical evolution of two-component clusters, with emphasis on the postcollapse phase. We study the relative importance of tidal capture and three-body binary formation for heating the cluster core. We are particularly interested in the importance of unequal stellar masses for gravothermal oscillations.

Our model is quite simple compared to real clusters. Stellar evolution has not been included; it is most important for the very early evolution of clusters (Chernoff & Weinberg 1990; Drukier 1995). Primordial binaries could be even more important than the binaries formed by dynamical processes through the early postcollapse phases (Gao et al. 1991), but we neglect them. We have ignored the tidal field of the galaxy, even though tidal limitation qualitatively alters postcollapse evolution of the cluster mass and radius (Hénon 1961; Lee & Goodman 1995), and tidal shocks may further hasten the destruction of clusters (Kundic & Ostriker 1995; Gnedin & Ostriker 1997). External tidal fields are probably not important for gravothermal oscillations and other phenomena pertaining to the core, except insofar as they modify the total cluster mass.

This paper is organized as follows: in §2 we describe the models and methods of our calculations. Heating mechanisms that derive the postcollapse expansion are compared in §3. In §4 we obtain a series of solutions and give simple analytic expressions for the evolution of parameters of postcollapse clusters. Gravothermal oscillation in two-component models is examined in §5. The final section summarizes our results.

2. MODELS

2.1. *Computational Method*

The dynamical evolution of collisionless stellar systems under the influence of two-body relaxation is well described by the Fokker-Planck equation. We have restricted ourselves to isotropic models, in which the stellar orbital distribution function depends only on energy (and time). A recent study by Takahashi, Lee, & Inagaki (1997) showed that the radial anisotropy in the halo becomes highly suppressed when a tidal field is imposed. The global evolution can be simply described by an isotropic model. The multicomponent Fokker-Planck equation can be written as follows:

$$4\pi^2 p(E)\,\frac{\partial f_i(E)}{\partial t} = -\,\frac{\partial F_i(E)}{\partial E}\,, \tag{1}$$

where $f_i(E)$ and $F_i(E)$ are the distribution function and the particle flux in energy space E, respectively, for the ith component. Formally F_i can be expressed as

$$F_i(E) = -m_i D_E f_i(E) - D_{EE}\,\frac{\partial f_i}{\partial E}\,, \tag{2}$$

where D_E and D_{EE} are the Fokker-Planck coefficients. The statistical weight factor $p(E)$ is given by

$$p(E) = 4\int_0^{\phi^{-1}(E)} r^2 v\,dr\,, \tag{3}$$

where $\phi^{-1}(E)$ denotes the maximum radius that a particle with energy E can reach in the spherical potential $\phi(r)$.

In order to account for the effects of binaries, we need to modify the above Fokker-Planck equation. Statler, Ostriker, & Cohn (1987) developed a sophisticated scheme to include the dynamical effects of tidal binaries for a model initially composed of a single component. Lee (1987) modified the method of Statler et al. (1987) to include both tidal binaries and three-body binaries. However, the number of dynamically produced binaries is always a very small fraction of the total number of stars. The most important effect is heating—the addition of entropy to the orbital distribution function—which can be simply accounted for by modifying the particle flux in energy space. Such an approach has been taken in many studies that deal with three-body binary heating (see, e.g., Cohn 1985; Lee, Fahlman, & Richer 1991). Normally the tidal binaries are more abundant, and a simple correction of the particle flux could cause some errors. However, we find that our approach provide excellent agreement with more complex schemes.

The orbit-averaged heating coefficient due to this heating becomes

$$H_i(E) = \frac{\int_0^{r_{\max}} \dot{E} v r^2\,dr}{\int_0^{r_{\max}} v r^2\,dr}\,, \tag{4}$$

where $\dot{E}$ is the heating rate per unit volume and $r_{\max}$ the maximum radius accessible to a star with energy E. The modified particle flux then takes the form

$$F_i(E) = -[m_i D_E + H_i(E)]f_i(E) - D_{EE}\,\frac{\partial f_i}{\partial E}\,. \tag{5}$$

The second-order coefficient D_{EE} is also affected by binary heating, but this diffusive effect is probably much less important for the long-term evolution than the change in D_E.

Heating by tidal binaries is mostly due to their ejection during close encounters with single stars (or sometimes other binaries) because the internal binding energy of tidal binaries is much greater than the escape energy from the cluster. Therefore the heating rate per unit volume is the product of the mass in all three stars, the binary formation rate, and the central potential (Lee & Ostriker 1993):

$$\dot{E}_{\rm tc} = (m_n + 2m_d)\sigma_{\rm tc}\, v_{\rm rel}\, n_n\, n_d\, \phi_c\,, \tag{6}$$

where n is the number density, $\sigma_{\rm tc}$ the tidal-capture cross section, $v_{\rm rel}$ the relative rms velocity between degenerate and normal stars, and ϕ_c the central gravitational potential. The subscript n denotes normal stars, while d represents degenerate stars. It is assumed that the binary is ejected promptly after formation by interaction with a third star. We adopt the following expression for $\sigma_{\rm tc}$ from Lee & Ostriker (1986) for tidal captures between a normal star and a degenerate star with $m_d/m_n = 2$:

$$\sigma_{\rm tc} = 13\left(\frac{v_{\rm rel}}{v_{e,n}}\right)^{-2.1} R_n^2\,, \tag{7}$$

where $v_{e,n}$ is the escape velocity at the normal star's surface and R_n is the normal star's radius.

Binaries formed by dissipationless three-body encounters ("three-body binaries") are usually less tightly bound than tidal binaries. Therefore, in their encounters with single stars, some or all of the stars are retained by the cluster and contribute their increased orbital energy to the distribution functions f_i ("direct heating"). Until ejected from the cluster, a three-body binary releases approximately 300 kT, where kT is the typical kinetic energy of background stars. Thus the three-body binary heating rate per unit volume

can be computed by multiplying the binary formation rate per unit volume by $300\,kT$:

$$\dot{E}_{3b} = 4.21 \times 10^3 G^5 \left(\sum_i \frac{n_i m_i^2}{v_i^3} \right)^3 v_c^2 , \quad (8)$$

where the summation is over all components, and v_c^2 is the mass-weighted, three-dimensional, central velocity dispersion. The numerical coefficient has been taken from Cohn (1985).

The modified Fokker-Planck equation can be accurately integrated with the numerical procedure described by Cohn (1979, 1980).

2.2. *Model Parameters*

Our models assume an initial cluster composed of main-sequence stars with mass m_1 and neutron stars with mass m_2. The total masses in the form of these stars are M_1 and M_2, respectively. The total number of stars is denoted by N.

We need to specify three dimensionless parameters in addition to the initial density and velocity profiles: the total number of stars N, the ratio m_2/m_1 of a heavy star to a light star, and the number ratio N_2/N_1. The dimensional scales are determined by the total cluster mass M, the initial half-mass radius $r_{h,i}$, and the stellar radius R_n. The ratio $m_1 r_{h,i}/MR_n$ is important for tidal heating because it determines the ratio of the capture cross section (eq. [7]) to the projected area of the cluster (or cluster core).

The present study may be divided into three topics, and each topic has its own set of models. The detailed model parameters of those sets are listed in Tables 1, 3, and 4. Note that in all our runs, the total mass of the heavy component, $M_2 \equiv N_2 m_2$, is negligible compared to the total mass of the light component, $M_1 \equiv N_1 m_1$, and thus $m_1 \approx M/N_1$. The initial density and velocity profiles are given by Plummer models with $v_{c1}/v_{c2} = 1$, and $\rho_{c1}/\rho_{c2} = M_1/M_2$, where ρ_c is the core density. Both three-body binary heating and tidal binary heating are included, and clusters are assumed to be isolated (i.e., no tidal cutoff).

Our values for m_2/m_1 range from 2 to 5. If we identify m_1 with the heaviest main-sequence stars, then $m_2/m_1 = 2$ is a suitable choice. Since the bulk of the cluster consists of stars below the turnoff, however, m_1 should be somewhat smaller than the turnoff-point mass. Finally, we assume a linear mass-radius relation, such that $1\,M_\odot$ corresponds to $1\,R_\odot$.

3. HEATING MECHANISMS

Most heating takes place in the core, where the stellar and binary number densities are highest. To compare the efficiencies of heating mechanisms, we first derive their dependence on core parameters. From equations (6) and (8), $\dot{E}_{\rm tc}$ in the core is approximately proportional to $v_n n_n n_d$, while $\dot{E}_{3b}$ in a core dominated by degenerate stars is approximately proportional to $n_d^3 v_d^{-7}$. We have assumed that $\phi_c \propto v_{n,c}^2$, which is valid during the postcollapse phase. Even during the precollapse phase, the ratio of potential depth to central velocity dispersion varies very slowly compared to other quantities. Considering again the fact that the core is dominated by degenerate stars, the central heating rate by tidal binaries is proportional to the first power of the central density, and the central heating rate by three-body binaries is proportional to the third power. Since the central velocity dispersion evolves much less than the central density, the density of degenerate stars in the core is the most important quantity in deciding the relative efficiency of the two heating mechanisms. Thus the relative importance of three-body binaries increases as the core collapse proceeds.

We have searched for the division of tidal and three-body heating dominance in the two-component parameter space, and its result is shown in Table 1, where 3B denotes the models whose postcollapse expansion is driven by three-body binaries, and TB those driven by tidal binaries. Three-body binary heating is relatively more important for clusters with smaller M and N_1/N_2, and larger $r_{h,i}$ and m_2/m_1. Smaller N_1/N_2 and larger m_2/m_1 give larger initial n_{c2}/n_{c1}, which is favorable to three-body binary formation. On the other hand, a cluster with very high initial n_i starts its evolution with tidal binary heating rate high enough not to give a chance for three-body binary heating to be dominant during the collapse. Kim & Lee (1997) found that the evolution of multicomponent models with various power-law mass functions and M may be realized with two-component models with $1.7 < m_2 < 3$ and $10 < N_1/N_2 < 50$ (the actual fraction of neutron stars in globular clusters is much less than 1/100, but many low-mass normal stars do not contribute much on the cluster's dynamical evolution). Although the dominant heating mechanism is dependent on the mass function (m_2/m_1 and N_1/N_2), all models with typical globular cluster masses and sizes ($M \lesssim 10^6\,M_\odot$ and $r_{h,i} \gtrsim 2.5$ pc) and with the above mass function range are dominated by three-body binary heating in the postcollapse phase as in Figure 1, which is a typical history of the heating rates of our models marked with 3B in Table 1. This dominance of 3B over TB in most plausible parameter range confirms the conclusion of Lee (1987) that in multicomponent clusters, three-body binary heating is relatively more important because there are no tidal captures between pairs of degenerate stars. Note that, even for an extreme N_1/N_2 value of 300, three-body binary heating is still dominant for clusters with $M \leq 3 \times 10^5\,M_\odot$ and $r_{h,i} \geq 5$ pc, which are the parameter ranges that the majority of the present clusters have.

Although tidal binary heating is unimportant for postcollapse expansion of models marked with 3B, tidal binary heating becomes more important when M and N_1/N_2 are larger, and when $r_{h,i}$ and m_2/m_1 are smaller. For example, our two-component model with $M = 10^6\,M_\odot$, $r_{h,i} = 2.5$ pc, $m_2/m_1 = 2$, $N_1/N_2 = 300$, and $m_2 = 1.4\,M_\odot$ is governed by tidal binary heating in the postcollapse phase (see Fig. 2). It is notable, however, that the three-body binary heating rate

TABLE 1

DOMINANT HEATING MECHANISM IN THE POSTCOLLAPSE PHASE

M ($M_\odot$)	$r_{h,i}$ (pc), $N_1/N_2 = 30$				$r_{h,i}$ (pc), $N_1/N_2 = 300$			
	1	2.5	5	10	1	2.5	5	10
$m_2/m_1 = 2$:								
1×10^5.....	3B	3B	3B	3B	TB	3B	3B	3B
3×10^5.....	3B	3B	3B	3B	TB	TB	3B	3B
1×10^6.....	TB	3B	3B	3B	TB	TB	TB	TB
3×10^6.....	TB	TB	3B	3B	TB	TB	TB	TB
$m_2/m_1 = 3$:								
1×10^5.....	3B	3B	3B	3B	3B	3B	3B	3B
3×10^5.....	3B	3B	3B	3B	3B	3B	3B	3B
1×10^6.....	3B	3B	3B	3B	TB	3B	3B	3B
3×10^6.....	3B	3B	3B	3B	TB	TB	TB	3B

NOTE.—3B denotes the models whose postcollapse expansion is driven by three-body binary heating, and TB those driven by tidal binary heating; $m_2 = 1.4\,M_\odot$ for all models.

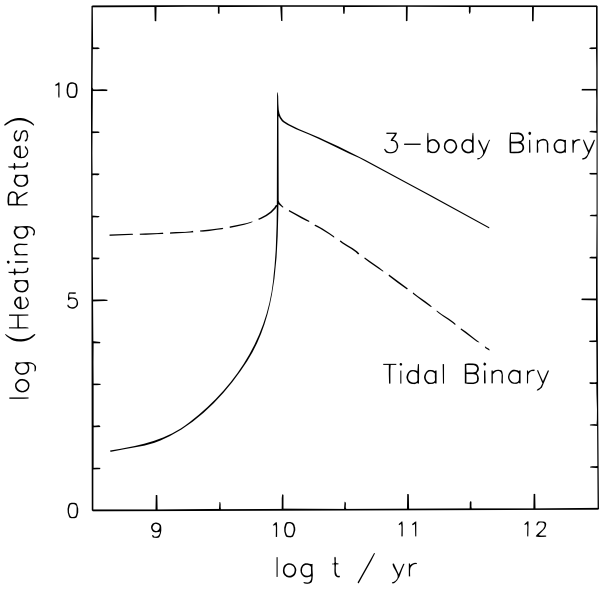


FIG. 1.—Heating rates by three-body binaries (*solid line*) and tidal binaries (*dashed line*) of run caab. Units of the *y*-axis are arbitrarily chosen.

increases after core collapse,while the rate of heating by tidal binaries decreases. This phenomenon is not expected for single-mass tidal binary–driven postcollapse clusters, in which the central density and velocity dispersion evolve as $\rho_c \propto t^{-1.04}$ and $v_c \propto t^{-0.34}$ (Lee & Ostriker 1993), and the three-body binary heating rate as $\rho_c^3 v_c^{-7} \propto t^{-0.8}$. In a two-component postcollapse cluster, however, if tidal binaries dominate and equipartition holds in the core, then the central density decreases less rapidly and the central velocity more rapidly than in a single-component cluster (Fig. 3). In such cases, the heating rate by three-body binaries may even increase during postcollapse expansion.

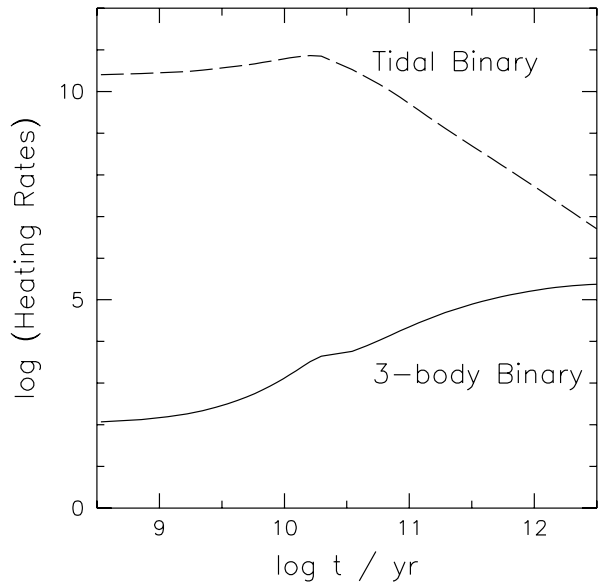


FIG. 2.—Heating rates by three-body binaries (*solid line*) and tidal binaries (*dashed line*) of our two-component model with $M = 10^6\ M_\odot$, $r_{h,i} = 2.5$ pc, $m_2/m_1 = 2$, $N_1/N_2 = 300$, and $m_2 = 1.4\ M_\odot$. Units of the *y*-axis are arbitrarily chosen. Initial tidal binary heating rate is so high that the three-body binary heating does not have a chance to take over. However, the three-body binary heating keeps increasing in the postcollapse phase.

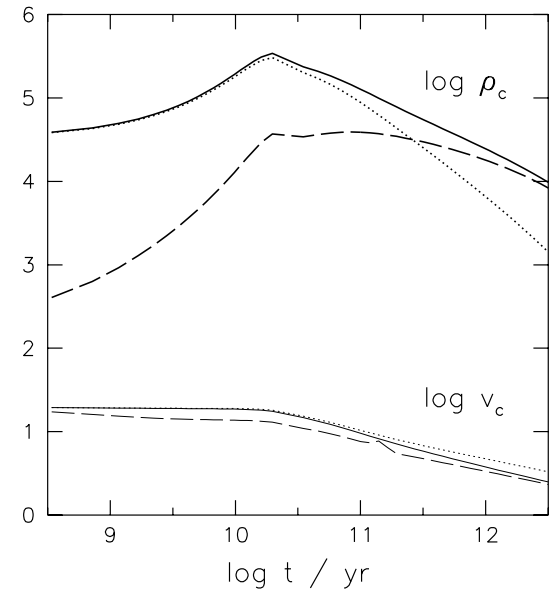


FIG. 3.—Temporal evolution of the core density (*thick lines*) and the central velocity dispersion (*thin lines*) for the same run as in Fig. 2. Dotted lines are for the light component, dashed lines for the heavy component, and solid lines for the overall values. Equipartition is approached in the postcollapse phase. ρ_c is in units of $M_\odot$ pc^{-3} and v_c in km s^{-1}.

The ultimate age of the models shown in Figures 1–4 appears unrealistically long. But the evolution of isolated clusters slows down as r_h expands (see § 3.3 below), whereas r_h, $t_{\rm rh}$, and M decrease during the postcollapse evolution of tidally limited clusters, which are more realistic (cf. Lee & Ostriker 1987). Thus, the evolutionary state of an isolated cluster at $t = 10^{11}$ yr roughly corresponds to that of a tidally limited one at a much earlier time. Mass loss by overflow of the tidal boundary is much more rapid than ejection of stars by binaries in the core and primarily depletes the lighter component. By decreasing N_1/N_2, this last effect further suppresses tidal binaries.

Many of the interactions that we identify as tidal captures would actually have led to mergers (Benz & Hills 1987). Ultimately, the mass of the normal star might still be ejected, but the neutron star would probably not be. Thus the parameter space for clusters whose postcollapse phase is driven by tidal binary heating is expected to be even more narrow than our present calculations suggest. As a limiting case, we have recalculated the two-component models in Table 1 assuming that the all tidal capture binaries end up

TABLE 2

DOMINANT HEATING MECHANISM IN THE POSTCOLLAPSE PHASE (MERGING CASE)

M ($M_\odot$)	$r_{h,i}$ (pc), $N_1/N_2 = 30$				$r_{h,i}$ (pc), $N_1/N_2 = 300$			
	1	2.5	5	10	1	2.5	5	10
$m_2/m_1 = 2$:								
1×10^5.....	3B	3B	3B	3B	3B	3B	3B	3B
3×10^5.....	3B	3B	3B	3B	TB	3B	3B	3B
1×10^6.....	3B	3B	3B	3B	TB	TB	3B	3B
3×10^6.....	3B	3B	3B	3B	TB	TB	TB	TB
$m_2/m_1 = 3$:								
1×10^5.....	3B	3B	3B	3B	3B	3B	3B	3B
3×10^5.....	3B	3B	3B	3B	3B	3B	3B	3B
1×10^6.....	3B	3B	3B	3B	3B	3B	3B	3B
3×10^6.....	3B	3B	3B	3B	TB	3B	3B	3B

NOTE.—Notation and m_2 are the same as in Table 1.

with mergers and only the masses of the normal stars are ejected, i.e.,

$$\dot{E}_{\rm tc} = m_n \sigma_{\rm tc} v_{\rm rel} n_n n_d \phi_c \ . \quad (9)$$

The dominant heating mechanism in the postcollapse phase for the models in Table 1 with the above $\dot{E}_{\rm tc}$ is shown in Table 2. The dominance of tidal binary heating is seen only for few models, because equation (9) gives $1/(2m_2/m_1 + 1)$ times less heating rate than equation (6), and thus three-body binaries now become even more important. For realistic mass functions ($N_1/N_2 \leq 50$), no model in our parameter range ($M \leq 3 \times 10^6$ and $r_{h,i} >$ pc) is marked with TB.

4. PRE- AND POSTCOLLAPSE EVOLUTION

In this section, we show the results for 11 models (group A). The parameters of these models, which are shown in Table 3, have been chosen to cover a range of plausible or instructive combinations. We now discuss some features of these models.

4.1. *Epoch of Core Collapse*

Isolated, single-component clusters beginning as Plummer models reach core collapse after a time $t_{\rm cc} = 15.4\ t_{{\rm rh},i}$ (Cohn 1980), where $t_{{\rm rh},i}$, the initial half-mass relaxation time, does not vary much before core collapse. However, the ratios $t_{\rm cc}/t_{{\rm rh},i}$ and $t_{\rm cc}/t_{\rm rc}$ (where $t_{\rm rc}$ is the core relaxation time) depend strongly on the initial density and velocity profile (Inagaki 1985), and can be much smaller for choices other than the conventional Plummer model. Quinlan (1996) found that for single-mass clusters, $t_{\rm cc}$ varies much less when expressed in units of $t_{\rm rc}$ divided by a dimensionless measure of the temperature gradient in the core. Single-mass clusters evolve by radial transport of energy, but energy exchange between different mass components plays an important role in multicomponent models. Mass segregation in a two-component model initially takes place on a timescale set by dynamical friction, which can be shorter than the core collapse time of a single-component model with similar macroscopic properties. Mass segregation and core collapse in two-component models has been discussed in detail by Inagaki (1985). In Table 3, we have listed the $t_{\rm cc}/t_{{\rm rh},i}$ ratios for each of our models.

4.2. *Scaling Laws for Postcollapse Evolution*

The expansion of the core in postcollapse is determined by the dominant heating mechanism. Here we present scaling laws for the postcollapse evolution of two-component clusters driven by three-body binary heating based on theoretical analysis and compare them with our numerical results (see Lee & Ostriker 1993 for scaling laws for evolution driven by tidal binary heating).

We start with Goodman's (1993) energy balance analysis arguments. The energy generation rate by three-body binaries in the core is

$$L_c \approx M_c \frac{\dot{E}_{3b,c}}{\rho_c} \ , \quad (10)$$

where the core mass M_c and core radius r_c are given by

$$M_c \equiv \frac{2\pi}{3} \rho_c r_c^3 \ , \quad (11)$$

$$r_c^2 \equiv \frac{3v_c^2}{4\pi G \rho_c} \ . \quad (12)$$

On the other hand, the power required by the expansion of the cluster is

$$\dot{E}_h \approx \frac{GM^2}{r_h^2} \dot{r}_h \ . \quad (13)$$

Since the heavy component dominates in the core and the light component at r_h, substitution of the core parameters into equation (8) yields

$$L_c \propto m_2^3 r_c^3 \rho_c^3 v_c^{-7} \ . \quad (14)$$

Slowly evolving postcollapse solutions are almost isothermal, and the core approaches equipartition. Thus the virial relation becomes

$$v_c^2 \approx v_{c2}^2 \approx \frac{m_1}{m_2} v_{c1}^2 \approx \frac{m_1}{m_2} \frac{GM}{r_h} \ . \quad (15)$$

Furthermore, the temporal dependence of the above parameters can be obtained from the assumption that

$$\frac{\dot{r}_h}{r_h} \propto \frac{1}{t_{\rm rh}} \ , \quad (16)$$

which would follow if the evolution were self-similar. Since $t_{\rm rh} \propto M^{1/2} m_1^{-1} r_h^{3/2}$, the above relation gives

$$(r_h^{3/2} - r_{h,{\rm cc}}^{3/2}) \propto \frac{m_1}{M^{1/2}} (t - t_{\rm cc}) \ , \quad (17)$$

where $r_{h,{\rm cc}}$ is r_h at $t = t_{\rm cc}$, and the outer part of the cluster is assumed to be dominated by the light component. Since r_h

TABLE 3

PARAMETERS AND RESULTS OF SIMULATION GROUP A

							Values at $t = 10^{11}$ yr			
Run	m_2/m_1	N_1/N_2	M ($M_\odot$)	N	m_2 ($M_\odot$)	$t_{\rm cc}/t_{{\rm rh},i}$	ρ_c ($M_\odot$ pc^{-3})	v_c (km s^{-1})	r_c (pc)	r_h (pc)
baab	2	100	10^5	141,457	1.4	12.42	1.47×10^5	3.03	0.0579	28.8
caab	3	100	10^5	210,125	1.4	6.34	1.29×10^5	2.86	0.0585	21.2
faab.....	4	100	10^5	277,473	1.4	3.23	1.19×10^5	2.80	0.0594	19.9
cdab	3	30	10^5	201,299	1.4	3.97	1.26×10^5	2.90	0.0600	28.6
cbab	3	300	10^5	212,871	1.4	10.92	1.26×10^5	2.85	0.0587	21.5
caab1	3	100	10^5	70,042	3×1.4	6.47	3.18×10^3	2.08	0.270	40.9
caab2	3	100	10^5	630,374	$1/3 \times 1.4$	6.28	5.36×10^6	3.91	0.0124	11.4
baab3.....	2	100	10^5	212,185	$2/3 \times 1.4$	12.17	6.10×10^5	3.40	0.0319	22.7
faab3	4	100	10^5	208,104	$4/3 \times 1.4$	3.23	4.57×10^2	2.58	0.0884	23.5
caeb	3	100	3×10^4	63,037	1.4	6.34	2.21×10^3	1.35	0.210	29.5
cabb	3	100	3×10^5	630,374	1.4	6.43	5.61×10^6	5.68	0.0176	15.9

NOTE.—The initial half-mass radii $r_{h,i}$ of these runs are all 5 pc.

is almost constant until the core collapse takes place,

$$(r_h^{3/2} - r_{h,i}^{3/2}) \propto \frac{m_1}{M^{1/2}} (t - t_{cc}) , \quad (18)$$

and for $t \gg t_{cc}$

$$r_h^{3/2} \propto \frac{m_1}{M^{1/2}} t . \quad (19)$$

It follows from equations (16) and (13) that

$$\dot{E}_h \propto m_1 M^{3/2} r_h^{-5/2} . \quad (20)$$

Demanding that the power (eq. [20]) required by expansion be supplied by the core luminosity (eq. [14]), and substituting for r_h from equation (19), one finds the following relations for late postcollapse evolution (i.e., $t \gg t_{cc}$):

$$\rho_c \propto \left(\frac{m_2}{m_1}\right)^{-10/3} N^{10/3} t^{-2} , \quad (21a)$$

$$v_c \propto \left(\frac{m_2}{m_1}\right)^{-1/2} N^{1/3} M^{1/3} t^{-1/3} , \quad (21b)$$

$$r_c \propto \left(\frac{m_2}{m_1}\right)^{7/6} N^{-4/3} M^{1/3} t^{2/3} , \quad (21c)$$

$$r_h \propto N^{-2/3} M^{1/3} t^{2/3} , \quad (21d)$$

$$M_c \propto \left(\frac{m_2}{m_1}\right)^{1/6} N^{-2/3} M . \quad (21e)$$

It is notable that $r_{h,i}$, one of the initial parameters of the cluster, is not included anywhere in equation (21). This, too, is a reflection of the self-similar nature of postcollapse evolution, which has been confirmed by many previous studies, but mostly for a single-mass component. Tidally limited postcollapse evolution, on the other hand, is not strictly self-similar, since r_c/r_h increases with decreasing cluster mass.

Unlike tidal binary heating, the calculation of three-body binary heating can be done purely dimensionlessly and is scalable to isolated clusters of any initial size, mass, and density. We can fix all of the constants in the scalings above from our numerical experiments:

$$\rho_c \simeq 4.5 \times 10^5 \, M_\odot \, \mathrm{pc}^{-3} \left(\frac{m_2}{m_1}\right)^{-10/3} N_5^{10/3} t_{11}^{-2.0} , \quad (22a)$$

$$v_c \simeq 3.8 \, \mathrm{km \, s^{-1}} \left(\frac{m_2}{m_1}\right)^{-1/2} N_5^{1/3} M_5^{1/3} t_{11}^{-0.32} , \quad (22b)$$

$$r_c \simeq 0.042 \, \mathrm{pc} \left(\frac{m_2}{m_1}\right)^{7/6} N_5^{-4/3} M_5^{1/3} t_{11}^{0.65} , \quad (22c)$$

$$r_h \simeq 35 \, \mathrm{pc} \, N_5^{-2/3} M_5^{1/3} t_{11}^{0.65} , \quad (22d)$$

$$M_c \simeq 71 \, M_\odot \left(\frac{m_2}{m_1}\right)^{1/6} N_5^{-2/3} M_5 \, t_{11}^{-0.05} , \quad (22e)$$

where $N_5 \equiv N/10^5$, $M_5 \equiv M/10^5 \, M_\odot$, and $t_{11} \equiv t/10^{11}$ yr. Note that the exponents of t, which are obtained by the power-law fitting, show only small discrepancies from equation (21).

The postcollapse central density evolutions of some of our runs with the same initial conditions and the same $N \times m_1/m_2$ values are shown in Figure 4. According to equation (21), these runs should have the same ρ_c at the same $t(>t_{cc})$, although their t_{cc}'s are different. After a short transition period in the beginning of the postcollapse phase, the ρ_c's do indeed converge to the same log-log slope.

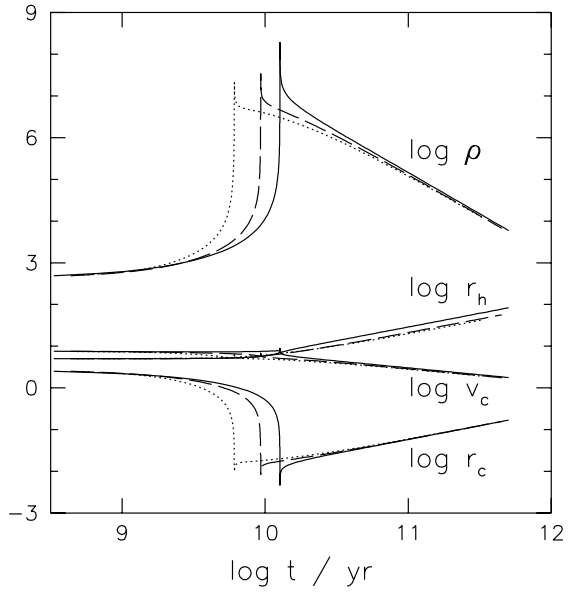


FIG. 4.—Temporal evolution of central densities, three-dimensional rms central velocities, core radii, and half-mass radii for runs baab (*solid line*), caab (*dashed line*), and faab (*dotted line*). These three runs have nearly the same $N \times m_1/m_2$ values and converge into the same evolutionary track in the postcollapse phase. ρ_c is in units of $M_\odot$ pc^{-3}, r_h and r_c in pc, and v_c in km s^{-1}.

Figure 5 shows ρ_c, v_c, r_c, and r_h of our runs in group A at $t = 10^{11}$ yr over the right-hand sides in equation (21). All panels in the figure have the same abscissa and ordinate scales, so that a slope of unity represents the proportions in equation (21). As one can see from these figures, our numerical results closely follow the scaling relationship. The best-fitting slopes in the figures are 1.02 ± 0.01, 0.92 ± 0.01, 1.07 ± 0.01, and 0.86 ± 0.06 for ρ_c, v_c, r_c, and r_h, respectively. These slopes are close to unity as represented by diagonal lines. The slope of r_h is the most discrepant. This is probably due to the approximations used in equations (16)–(19). The validity of equation (16) will be discussed again in § 5.

According to the scalings above, the central density depends upon the total mass M, on the epoch t, and on m_2, but it is independent of M_1 and M_2 separately. Therefore, the mass function does not influence the central density in postcollapse (provided that there are enough heavy stars to fill the core—see below), even though it strongly influences the epoch of core collapse.

The degree of concentration can be measured by r_h/r_c, which is constant during the postcollapse phase. From equations (22c) and (22d) we have

$$\frac{r_h}{r_c} = 833 \, N_5^{2/3} \left(\frac{m_1}{m_2}\right)^{7/6} . \quad (23)$$

In tidally limited postcollapse models, the tidal radius is larger than r_h by a factor of the order of 10. This means the concentration parameter of postcollapse cluster could become as large as 4. This is consistent with the fact that the stellar density profile of M15 obtained by the *Hubble Space Telescope* (*HST*) does not show a flat core down to 2″ (Guhathakurta et al. 1996). Note, however, that the core radius obtained from the light profile is somewhat larger than the core radius of the mass; more importantly, real

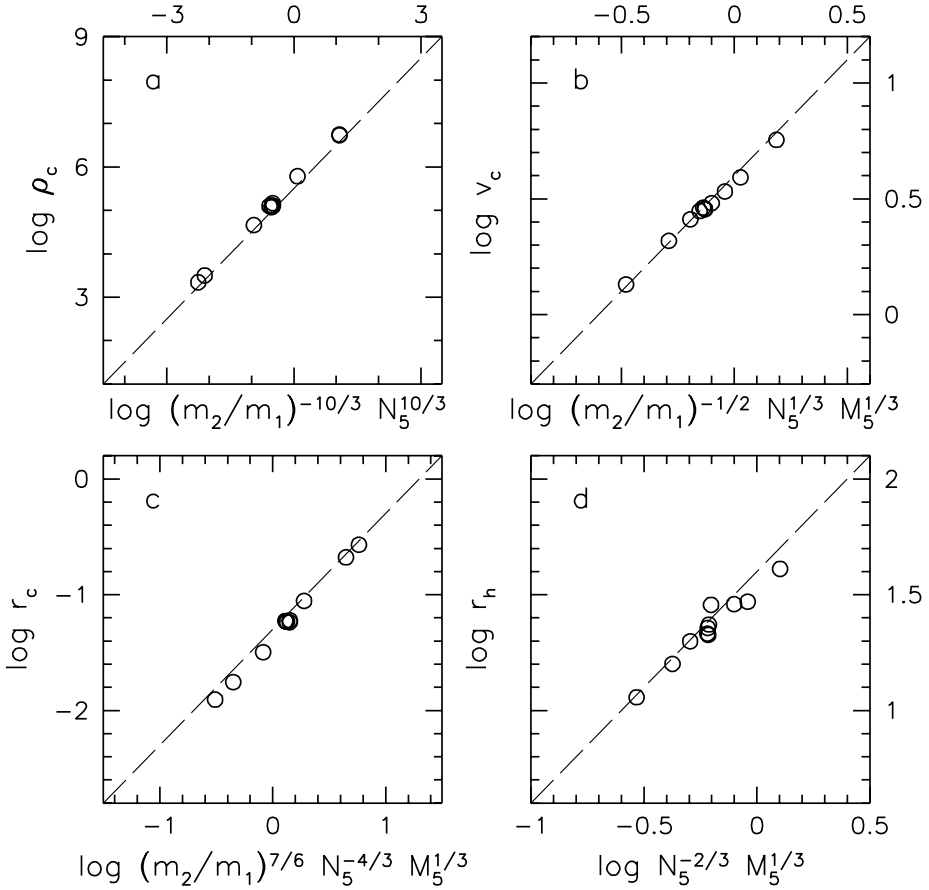


FIG. 5.—(*a*) Central densities, (*b*) three-dimensional rms central velocities, (*c*) core radii, and (*d*) half-mass radii of runs in group A. $N \equiv N/10^5$ and $M_5 \equiv M/10^5\ M_\odot$. The straight diagonal lines represent the theoretical relations.

clusters are tidally limited and are therefore not described accurately by these models.

5. GRAVOTHERMAL OSCILLATIONS

The inner regions of a slowly evolving postcollapse cluster are nearly isothermal. Their slow expansion on the timescale $t_{\rm rh}$ is almost negligible on the local timescale $t_{\rm rc}$. Thus these regions resemble equilibrium isothermal spheres and are therefore subject to the gravothermal instability studied by Antonov (1962) and Lynden-Bell & Wood (1968). This instability of postcollapse clusters was first found by Sugimoto & Bettwieser (1983) and Bettwieser & Sugimoto (1984) and later investigated by a number of scientists.

5.1. *The Instability Parameter* ϵ

Single-component, isolated clusters in postcollapse form a one-parameter family when they are dominated by three-body binaries. That parameter can be taken to be N, the number of stars. In this case, gravothermal instability occurs for $N \lesssim N_{\rm crit} \approx 7000$ (Goodman 1987). The introduction of multiple components brings additional dimensionless parameters, which affect the energy-generation rate in the core and perhaps also the relaxation rate near r_h. We may therefore expect that the instability should depend on parameters other than N.

Goodman (1993) suggested that the quantity

$$\epsilon \equiv \frac{E_{\rm tot}/t_{\rm rh}}{E_c/t_{\rm rc}} \tag{24}$$

should describe the degree of stability universally (regardless of the presence of mass spectrum), where

$$E_c \equiv \frac{2\pi}{3}\,\rho_c\, r_c^3\, v_c^2 \tag{25}$$

is the energy of the core, and $t_{\rm rh}$ and $t_{\rm rc}$ are half-mass and core relaxation times, respectively. The motivation for this idea is that the core luminosity L_c is stabilizing: equations (12) and (14) indicate that L_c will increase as the core shrinks and decrease as it expands. The stabilizing influence will be ineffective if $\epsilon \ll 1$, however, because then the "equilibrium" luminosity of the core ($\propto E_{\rm tot}/t_{\rm rh}$) is very small compared to the rate at which heat can be removed from the core if isothermal conditions should break down ($\propto E_c/t_{\rm rc}$).

Our two-component models provide a test of these ideas, since, as Goodman (1993) argued, ϵ depends both on N and on m_2/m_1. We have performed another set of runs (group B), whose parameters were chosen to test the analytical predictions given below. These simulations include heating by three-body binaries only. The initial conditions were Plummer models with three different mass ratios ($m_2/m_1 =$ 1.5, 2, 3) and four different total numbers ($N = 3 \times 10^4$, 1×10^5, 3×10^5, 1×10^6). We have fixed $N_1/N_2 = 100$ except for four supplementary runs. The parameters of the Group B runs are shown in Table 4.

As in Table 4 and Figure 6, six out of 12 runs showed gravothermal oscillations in the postcollapse expansion phase. Figure 7 shows that ϵ itself oscillates. An "equilibrium" value for ϵ can be obtained by adopting inte-

TABLE 4

PARAMETERS AND RESULTS OF SIMULATION GROUP B

Run	m_2/m_1	N_1/N_2	N	ϵ	r_c/r_h	Oscillation?
go01	1.5	100	3×10^4	1.09×10^{-2}	4.09×10^{-3}	n
go02	2.0	100	3×10^4	2.40×10^{-2}	7.03×10^{-3}	n
go03	3.0	100	3×10^4	5.96×10^{-2}	1.31×10^{-2}	n
go04	1.5	100	10^5	4.97×10^{-3}	1.69×10^{-3}	y
go05	2.0	100	10^5	1.08×10^{-2}	2.94×10^{-3}	n
go06	3.0	100	10^5	2.53×10^{-2}	5.38×10^{-3}	n
go07	1.5	100	3×10^5	2.13×10^{-3}	6.47×10^{-4}	y
go08	2.0	100	3×10^5	4.61×10^{-3}	1.13×10^{-3}	y
go09	3.0	100	3×10^5	1.12×10^{-2}	2.33×10^{-3}	n
go10	1.5	100	10^6	7.73×10^{-4}	2.09×10^{-4}	y
go11	2.0	100	10^6	1.80×10^{-3}	4.25×10^{-4}	y
go12	3.0	100	10^6	4.08×10^{-3}	8.23×10^{-4}	y
Supplementary runs:						
go05a	2.0	30	10^5	0.97×10^{-2}	2.70×10^{-3}	y
go05b	2.0	300	10^5	0.90×10^{-2}	2.57×10^{-3}	n
go08a	2.0	30	3×10^5	3.98×10^{-3}	1.05×10^{-3}	y
go08b	2.0	300	3×10^5	4.15×10^{-3}	1.05×10^{-3}	y

NOTE.—ϵ and r_c/r_h values are equilibrium values.

gration time steps larger than the typical oscillation period; with the implicit time integration schemes that we and others use, large time steps suppress the gravothermal oscillations. The equilibrium ϵ is almost constant during the whole instability period (Fig. 7) and can be used as a representative value for the postcollapse phase. These representative ϵ's are plotted in Figure 6 against a combination of cluster parameters that will be explained in the following subsection. There is a clear boundary of stability at $\epsilon_{\rm crit} \approx 0.01$, close to the value 0.013 found by Goodman (1993) for single-component clusters.

It is instructive to compare certain rows in Table 2. Runs go04, go05, and go06 have the same number of stars in the heavier component but increasing values of m_2/m_1, ϵ, and r_c/r_h. The first run shows oscillations, and the latter two do not. Therefore, the suggestion of Murphy, Cohn, & Hut (1990) that stability depends on the number of heavy stars is not borne out by these runs. Note, by the way, that the number of heavy stars is only 1000, much less than the critical value for instability in single-mass clusters (7000). It is also interesting to compare the unstable run go04 with run go09: the latter has 3 times as many stars in each component but is stable, apparently because of its larger m_2/m_1.

5.2. *Dependence of ϵ on Cluster Parameters*

In their study on the stability of clusters with three-body binaries and a broad mass spectrum, Murphy et al. (1990) found that stability persists to much larger N than in single-mass clusters, if the mass function is steep. They suggested that stability depends mainly on the total number of the heaviest stars. We believe that $\epsilon \lesssim 0.01$ is a more reliable criterion for the onset of instability.

We now determine ϵ as a function of cluster parameters. We derive simple scaling relations by analytic arguments and compare the results with our numerical results.

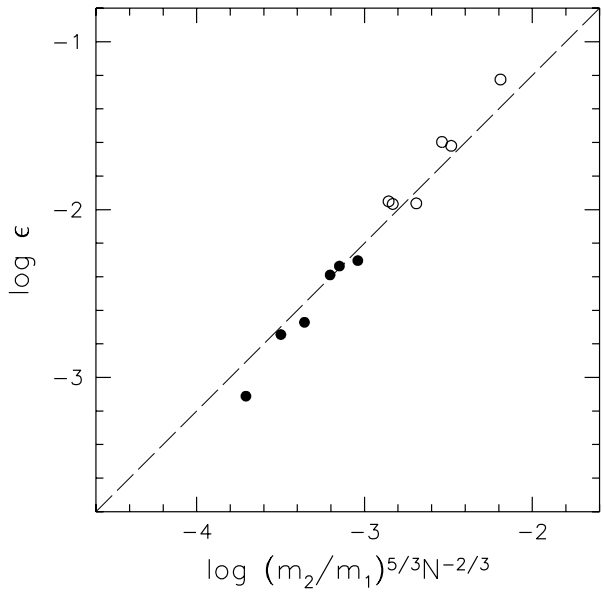


FIG. 6.—Oscillation-suppressed ϵ values of runs in group B. Filled circles are for runs that showed gravothermal oscillation, and open circles are for those that did not. There is a boundary near $\epsilon \simeq 0.01$ below which oscillations take place. The diagonal straight line represents the simple scaling relation in eq. (29).

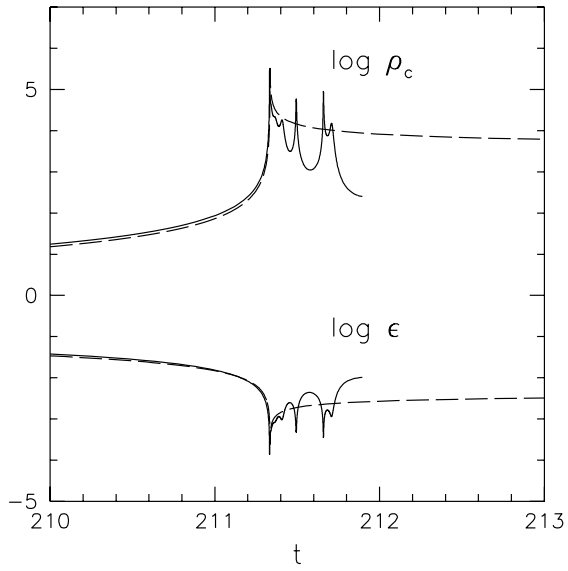


FIG. 7.—Comparison of oscillation-suppressed (*dashed lines*) and unsuppressed (*solid lines*) evolution of central density (*upper lines*) and ϵ (*lower lines*) of run go12. The oscillation-suppressed values are obtained by appropriately enlarging integration time steps for the Fokker-Planck equation. The oscillation-suppressed values for ϵ are good (and almost constant) representatives of ϵ during oscillation. ρ_c is in units of $10^5\ M_\odot$ pc^{-3} and t in code units ($\simeq t_{{\rm rh},i}$).

First we reproduce the prediction by Goodman (1993). From equation (21), one obtains

$$\left(\frac{r_c}{r_h}\right) \propto \left(\frac{m_2}{m_1}\right)^{7/6} N^{-2/3} . \tag{26}$$

Now, from equations (11), (12), and (15), the ratio of energies in the cluster and the core is

$$\frac{E_{\rm tot}}{E_c} \propto \frac{M}{M_c}\frac{v_m^2}{v_c^2} \propto \frac{r_h}{r_c}\frac{v_m^4}{v_c^4} , \tag{27}$$

where v_m^2 is the velocity dispersion of the whole cluster. Similarly, the ratio of half-mass to core relaxation time is

$$\frac{t_{\rm rh}}{t_{\rm rc}} \propto \frac{M^{1/2}}{M_c^{1/2}}\frac{r_h^{3/2}}{r_c^{3/2}}\frac{\bar{m}_c}{\bar{m}} \propto \frac{r_h^2}{r_c^2}\frac{v_m}{v_c}\frac{\bar{m}_c}{\bar{m}} , \tag{28}$$

where $\bar{m}$ is the mean mass in the cluster, and $\bar{m}_c$ is the mean mass in the core. With $\bar{m}_c/\bar{m} \approx m_2/m_1$ and $v_m^2/v_c^2 \approx m_2/m_1$, one finally obtains

$$\epsilon \propto \left(\frac{r_c}{r_h}\right)\left(\frac{m_2}{m_1}\right)^{1/2} \propto \left(\frac{m_2}{m_1}\right)^{5/3} N^{-2/3} . \tag{29}$$

The exponents of mass ratio 3/2 and 2 in equation (18) of Goodman (1993) should be corrected to 7/6 and 5/3 as in equations (26) and (29).

We have compared the above scaling relations with our numerical results from runs in group B. The equilibrium ϵ values of our runs are plotted in Figure 6 against the right-hand side of equation (29). The data points are well aligned, and their slope is 1.20 ± 0.05, slightly higher than the theoretical value of unity.

This discrepancy is traceable to the deviation of r_c/r_h from the predicted scaling (eq. [26]). In § 4 we remarked that our numerical results show a slightly higher slope than expected for r_c (1.07 ± 0.01 vs. 1) and a lower slope for r_h (0.86 ± 0.06 vs. 1). Thus the slope for r_c/r_h should be higher than predicted by our analytic arguments by appproximately 0.21 for the runs in group A. The correlation between the two sides of equation (26) for group B is shown in Figure 8. The slope of these data points is 1.26 ± 0.04, which is comparable to the one for ϵ. We find that one of the causes of this poor r_c/r_h approximation is the assumption that the proportionality constant in equation (16) is independent of cluster parameters. However, we find that the ratio $(r_h/t_{\rm rh})/\dot{r}_h$ of our runs ranges from 10 to 15. Runs with larger m_2/m_1 show larger $(r_h/t_{\rm rh})/\dot{r}_h$ values, and this m_2/m_1 dependence is more pronounced for runs with larger N. If one lets

$$\frac{r_h}{t_{\rm rh}} \equiv A\dot{r}_h , \tag{30}$$

where the coefficient A depends on cluster parameters, such as m_2/m_1 and N, one finds

$$r_c/r_h \propto A^{8/9} . \tag{31}$$

Then a 23% variation in A would give a 20% residual in the slope of the correlation between the two sides of equation (16). This is approximately what one sees in Figure 8, which is based on m_2/m_1 ranging from 1.5 to 3. Although equation (16) has been widely used without consideration of its dependence on cluster parameters, we conclude that the coefficient in this relation varies with the mass function.

We have made four more runs in addition to group B to test the dependence of ϵ on N_1/N_2, which is not apparent in equation (29): two runs with the same parameters as run go05 except $N_1/N_2 = 30$ and 300 (go05a and go05b, respectively), and two runs as run go08 except $N_1/N_2 = 30$ and 300 (go08a and go08b, respectively). Equilibrium ϵ values of these runs are 0.97×10^{-2} for run go05a, 0.90×10^{-2} for run go05b, 3.98×10^{-3} for run go08a, and 4.15×10^{-3} for run go08b. These values are all within only 15% differences from their comparison runs, go05 and go08, indicating that ϵ is independent of N_1/N_2 as expected in the above energy balance analysis. However, while gravothermal oscillations are observed in run go08a and not in runs go05a and go05b as expected, they are not observed in run go08b. Clearly the criterion of $\epsilon \gtrsim 0.01$ does not appear to be exact if N_2 is too small.

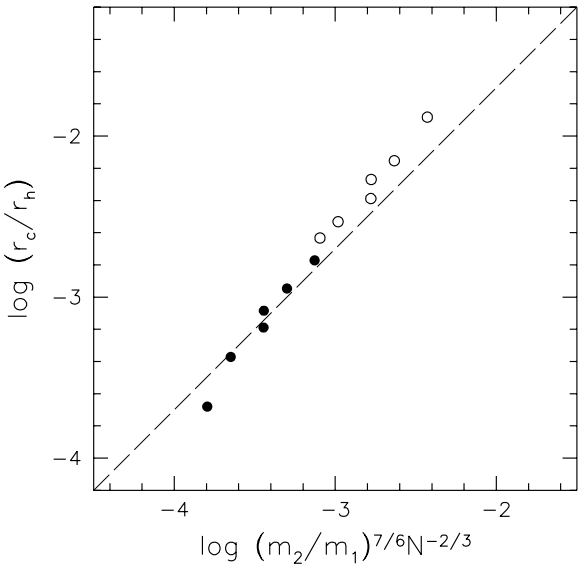


FIG. 8.—Oscillation-suppressed r_c/r_h values of our runs in group B. Filled circles are for runs that showed gravothermal oscillation, and open circles are for those that did not. The straight diagonal line represents the theoretical scaling relation.

All of our previous analyses assume that there are enough stars in the heavy component so that the core is dominated by them. This requires that the ratio of core mass to total mass,

$$\frac{M_c}{M} \approx 3.3\left(\frac{m_2}{m_1}\right)^{1/6} N^{-2/3} t_{11}^{-0.05} \tag{32}$$

(see eq. [22e]) should be smaller than M_2/M. In order to confine most of the heavy stars to a region much smaller than r_h, we also require $m_2/m_1 > 3/2$: $\rho_2(r) \propto \rho_1(r)^{m_2/m_1}$ in equipartion; $\rho_1 \propto r^{-2}$ in the regions well outside the core where the lighter component dominates the potential; and we require $\rho_2(r)$ to fall more steeply than r^{-3} in those regions so that most of the heavies are at smaller radii. All of our runs satisfy these requirements, except where $m_2/m_1 = 1.5$ so that the second condition is marginally violated.

6. SUMMARY

We have investigated the evolution of isolated two-component clusters with Plummer model initial conditions. We have included the main effects of both three-body and tidal-capture binaries by adding a heating term to the Fokker-Planck equation.

In agreement with previous investigators, we find that core collapse is hastened by the presence of heavy remnant stars.

In the postcollapse phase, we find that heating by three-body binaries exceeds that by tidal binaries at least for clusters with $M \leq 3 \times 10^5\ M_\odot$, $r_{h,i} \geq 5$ pc, $m_2/m_1 \geq 2$, and $N_1/N_2 \leq 300$ when $m_2 = 1.4\ M_\odot$. When three-body binary heating does dominate, the expansion of the postcollapse cluster is self-similar. Scaling laws for cluster parameters, including the central density, velocity dispersion, core radius, and half-mass radius, have been derived from simple considerations of energy balance, and these scalings generally agree well with our numerical results, which, however, also provide the numerical coefficients in the scaling laws. We related the postcollapse evolution of these cluster parameters to N, M, and m_1/m_2.

We have studied the gravothermal oscillation phenomenon using our two-component models. We have confirmed that the parameter $\epsilon = (E_{\rm tot}/t_{\rm rh})/(E_c/t_{\rm rh})$ predicts the occurrence of gravothermal oscillations in the presence of this simplest of nontrivival mass functions. The scaling law for ϵ with respect to m_1/m_2 and N is derived in the limit of small N_2/N_1 and compared with our numerical results. Generally speaking, clusters with a steeper mass function are less susceptible to gravothermal instability. This is in qualitative agreement with an earlier suggestion by Murphy et al. (1990), but whereas these authors suggested that stability depends on the number of heavy stars, we conclude that it is independent of the number of heavies but depends jointly on the total number of stars and on the ratio of the individual stellar masses in the two components.

These conclusions need to be tested against models with more mass components. Our preliminary studies indicate that the evolution of multimass clusters is generally similar to two-component models for an appropriate choice of model parameters (mostly suitable m_2/m_1). In order to compare with real clusters, we need to take into account a host of complicating physical effects, most importantly an external tidal field. The results of these studies will be reported elsewhere.

S. S. K. thanks Chang Won Lee and Jung-Sook Park for obtaining old and rare papers. This research was supported in part by Korea Science and Engineering Foundation, 95-0702-01-01-03, and in part by the Matching Fund Programs of the Research Institute for Basic Sciences, Pusan National University, RIBS-PNU-96-501.

REFERENCES

Antonov, V. A. 1962, Vest. Leningrad Univ., 7, 135 (English Transl. in IAU Symp. 113, Dynamics of Star Clusters, ed. J. Goodman & P. Hut [Dordrecht: Reidel], 525 [1985])
Benz, W., & Hills, J. G. 1987, ApJ, 323, 614
Bettwieser, E., & Sugimoto, D. 1984, MNRAS, 208, 493
Chernoff, D. F., & Weinberg, M. 1990, ApJ, 351, 121
Cohn, H. N. 1979, ApJ, 234, 1036
———. 1980, ApJ, 242, 765
———. 1985, in IAU Symp. 113, Dynamics of Star Clusters, ed. J. Goodman & P. Hut (Dordrecht: Reidel), 161
Drukier, G. A. 1995, ApJS, 100, 347
Gao, B., Goodman, J., Cohn, H., & Murphy, B. 1991, ApJ, 370, 567
Gebhardt, K., & Fischer, P. 1995, AJ, 109, 209
Gnedin, O. Y., & Ostriker, J. P. 1997, ApJ, 474, 223
Goodman, J. 1987, ApJ, 313, 529.
———. 1993, in ASP Conf. Ser. 50, Structure and Dynamics of Globular Clusters, ed. S. G. Djorgovski & G. Meylan (San Francisco: ASP), 87
Guhathakurta, P., Yanny, B., Schneider, D. P., & Bahcall, J. N. 1996, AJ, 111, 267
Hénon, M., 1961, Ann. d'Astrophys., 24, 369
Inagaki, S. 1985, in IAU Symp. 113, Dynamics of Star Clusters, ed. J. Goodman & P. Hut (Dordrecht: Reidel), 189
Inagaki, S., & Wiyanto, P. 1984, PASJ, 36, 391
Kim, S. S., & Lee, H. M. 1997, Publ. Korean Astron. Soc., 30(2), 115
Kulkarni, S. R., Hut, P., & McMillan, S. 1993, Nature, 364, 421
Kundic, T., & Ostriker, J. P. 1995, ApJ, 438, 702
Lee, H. M. 1987, ApJ, 319, 772
Lee, H. M., Fahlman, G. G., & Richer, H. B. 1991, ApJ, 366, 455
Lee, H. M., & Goodman, J. 1995, ApJ, 443, 109
Lee, H. M., & Ostriker, J. P. 1986, ApJ, 310, 176
———. 1987, ApJ, 322, 123
———. 1993, ApJ, 409, 617
Lynden-Bell, D., & Wood, R. 1968, MNRAS, 138, 495
Murphy, B. W., Cohn, H. N., & Hut, P. 1990, MNRAS, 245, 335
Phinney, E. S. 1993, in ASP Conf. Ser. 50, Structure and Dynamics of Globular Clusters, ed. S. G. Djorgovski & G. Meylan (San Francisco: ASP), 137
Quinlan, G. D. 1996, New Astron., 1, 255
Spitzer, L., Jr. 1987, Dynamical Evolution of Globular Clusters (Princeton: Princeton Univ. Press)
Statler, T. S., Ostriker, J. P., & Cohn, H. N. 1987, ApJ, 316, 626
Sugimoto, D., & Bettwieser, E. 1983, MNRAS, 204, 19P
Takahashi, K., Lee, H. M., & Inagaki, S. 1997, MNRAS, submitted
Yoshizawa, M., Inagaki, S., Nishida, M. T., Kato, S., Tanaka, Y., & Watanabe, Y. 1978, PASJ, 30, 279